ELSEVIER

Computerized Medical Imaging and Graphics 28 (2004) 203–211

Computerized Medical Imaging and Graphics

www.elsevier.com/locate/compmedimag

A digital reference model of the human bronchial tree

Andreas Schmidt[a], Stephan Zidowitz[b], Andres Kriete[a,*], Thorsten Denhard[a], Stefan Krass[b], Heinz-Otto Peitgen[b]

[a]*Image Processing Laboratory, Institute of Anatomy and Cell Biology, Justus-Liebig-University, Aulweg 123, 35385 Giessen, Germany*
[b]*Center for Medical Diagnostic Systems and Visualization (MeVis), Universitätsallee 29, 28359 Bremen, Germany*

Received 10 July 2003; accepted 23 December 2003

Abstract

In-vitro preparations of the human lung combined with high-resolution tomography can be used to derive precise models of the human lung. To develop an abstract graph representation, specially adapted image processing algorithms were applied to segment and delineate the bronchi. The graph thus obtained contains topological information about spatial coordinates, connectivities, diameters and branching angles of 1453 bronchi up to the 17th Horsfield order. The graph was analyzed for statistical and fractal properties and was compared with current models. Results indicate a model that exhibits asymmetry and multifractal properties. This newly established reference model is an important step forward in geometrical accuracy of the bronchial tree representation that will improve both analysis of lung images in clinical imaging and the realism of functional simulations.

Keywords: Bronchial tree; Lung preparation; High-resolution computer tomography; Lung modeling

1. Introduction

A widely-used model for simulations and predictions of gas transport, particle deposition and dosimetry is that of a regular, dichotomic branching pattern [1–4], a representation that has its origin in the so-called trumpet model [5] that is used with geometric adjustments introduced later [6]. This is a simplification of the lung geometry that assumes a spatially symmetric branching, a fixed relation of the cross-sections of a parent branch with the daughter branches, and a constant length of all possible spatial trajectories between the trachea and any terminating bronchioli. This model is self-similar regarding spatial scaling properties and as such it reveals fractal properties.

Even though the human bronchial tree, at least for the first six generations, exhibits a most symmetrical branching if compared to a wide variety of species, irregular and asymmetric branching pattern cannot be neglected [7–9]. Therefore, regular symmetric models do not predict gas flow and particle deposition reliably, and more realistic models are needed to increase accuracy. Dichotomic branching models also tend to fill space in a spheric fashion and can not be adapted to the form and volume of the human lung [3].

For the local analysis of air flows, more sophisticated models are in use to show that many of the transport processes within the airways depend quite sensitively on the geometry of the bronchial bifurcations and the structure of the boundaries [10–12]. But in the global modelling of the tracheobronchial tree, recent efforts rely on stochastic models [13,14] or synthesize the underlying structure from fixed scaling laws [4,15,16] based on a small number of anatomic examinations. These models meant to represent a mean adult lung, rather than describing the lung of a specific individual.

We present the development of a digital reference model of the bronchial tree of a normal lung that is based on high-resolution computer tomography (HRCT) imaging of an in-vitro preparation. The image data are suitable for an in-depth computer-based investigation of the branching pattern of the bronchial tree and statistical analysis of geometry. A new reference model is derived, which will allow further improvements of functional simulations including particle transport and digital dosimetry.

* Corresponding author. Address: School of Biomedical Engineering, Science and Health Systems, Drexel University, 3141 Chestnut Street, Philadelphia, PA 19104-2875. Tel.: +1-215-895-2215; fax: +1-215-895-4983.

0895-6111/$ - see front matter © 2004 Elsevier Ltd. All rights reserved.
doi:10.1016/j.compmedimag.2004.01.001

2. Materials and methods

2.1. Imaging and image analysis

Data were provided from a human lung of an adult male, free of pathological alterations [17], excised at autopsy and fixed (Institute of Anatomy, Bern, Switzerland). A liquid rubber solution was injected into the lumen of the bronchial tree and into the lung vessels of one lobe. The rubber fixed the lumen of the bronchial tree in nearly end-inspiratory volume. After removal of the lung parenchyma and filled respiratory units, a set of digital volume data was produced by using high-resolution computed tomography, with a pixel dimension of $0.35 \times 0.35\ \text{mm}^2$ and with 0.4 mm distance between slices (GSF, Neuherberg, Germany). A representative example from this series is given in Fig. 1.

The bronchial tree was segmented from the HRCT volumetric data with a threshold-based algorithm, where the threshold is preselected automatically leading to an optimal segmentation result. Starting from a user defined seedpoint, the algorithm accumulates all high-intensity voxels above a defined threshold. An interactive correction of the automatically determined threshold was executed. Resultant we achieve a binary volume representation of the trachea and the connected bronchial tubes, with comprised the trachea down to the main stem bronchi. The grey value volume data as well as the binary segmentation result were edited under visual control to overcome minor imperfections of the rubber cast.

For the left side of the lung beside the bronchial tree, pulmonary arteries and veins are filled in the rubber cast as well. Hence, the extractable depth of the hierarchical structure of the bronchial tree is limited by the increasing difficulties to separate the bronchial tree from the vessels. To achieve a homogeneous model we reduce the segmented tree for both lung sides to the hierarchical order given by the result for the left lung. However, we use results with higher resolution of the right lung for cross-comparisons.

Based on the binary representation of the bronchial tree we obtained two different models for further calculation: a surface representation of the segmented volume of the bronchial tree (Fig. 2a) and a graph representation describing the branching topology, but also including information about the diameter and length of each branch. The resulting graph contains all information to reconstruct a simplified, tube-like surface representation of the geometry, as demonstrated in Fig. 2b.

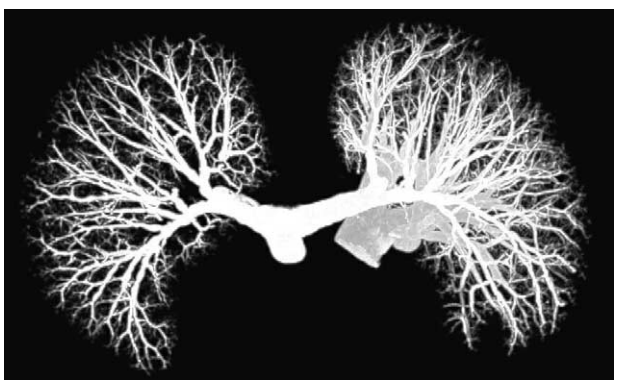

Fig. 1. Max-intensity projection of a 6 cm horizontal slab of the HRCT data displayed with inverted grey scale.

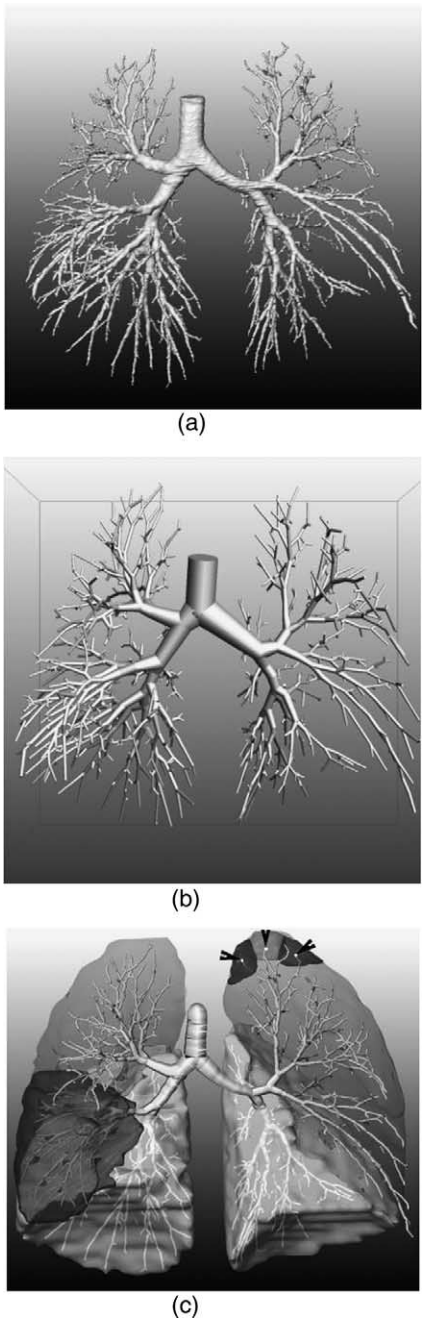

Fig. 2. 3D visualisation of bronchial tree models. (a) (upper): Surface representation of segmented volume data. Notice the regular patterns of imprints in the trachea and the primary bronchi that stem from cartilage rings. (b) (middle): Visualisation of a tube model reconstructed from an abstracted topological graph. (c) (lower): Visualisation of the synthetic generated lobe volumes along with the bronchial tree. Drain volumes attached to the marked leaves are added at the left lobe.

Surface extraction based on the binary volume data was established by a marching cube algorithm [18]. A volume preserving smoothing algorithm was applied to the resulting polygonal surface representation in order to reduce small-scale noise artefacts and discretisation artefacts in the data. The surface geometry can be exported into a special stereolitographic ('STL') data format to allow further processing with commercial grid generation packages.

In order to derive the graph presentation, the tubular structures were skeletonized. The implemented skeletonization method is based on a thinning algorithm and takes special care of anisometric voxel size and boundary noise, which yields exact centrelines representations [19–22]. During the erosion process, it is important to check whether the deletion of a particular voxel preserves the 3D topology of the object. For further analysis, the skeleton is interpreted as a graph, where the vertices represent ramification points of the medial axis and the edges represent the parts of the medial axis between the ramifications. The bronchi belonging to each lung segment were identified. Hereby, the skeleton is transformed in a directed acyclic graph with vertices representing branchings and edges representing connections between them. For each edge, a list is kept recording the skeleton voxels and vessel diameters along it. In a post-processing step, ambiguities were removed from the graph topology, including trifurcations and wrongly assigned groups of branches that are a consequence of noise at the object boundary. Distance transformation that evaluate the gradient along and perpendicular to the branches indicate the relevance of a side branch.

Further, we construct a model of the outer lung boundary by a morphological closing of the HRCT data followed by a smoothing of the resulting surfaces. For this purpose relevant structures in the HRCT data are defined by using a global threshold. The lung volume given hereby is split into regions for the lobes. Zones of reduced structure density in the HRCT data are identified as boundaries of the lobes therefore using watershed transform [23]. Assigning each point of the lung volume to the nearest terminating leaf of the segmented bronchial tree belonging to the same lobe we get an estimation for the drain volume supplied downstream by each part of the bronchial tree. In Fig. 2c a visualisation of the synthetically generated lobes is given. In the left upper lobe (LU) some resulting drain volumes attached to the leaves are shown.

The algorithms for image processing were implemented as modules under ILAB4 [24], a research and development platform for medical image processing and visualization developed at MeVis. Albeit specially adapted for the data of the cast, only minor changes are needed to apply the algorithms to the analysis of clinical radiological data of lung.

2.2. Statistical procedures and conventions

A number of different statistical evaluations were performed to describe the properties of the newly established geometric reference model. The model has a tree-like structure where the trachea is the 'stem' and the bronchi and bronchioles branch out from the trachea. This means the model is considered to be a bifurcating system: each parent branch, b_{parent}, gives rise to two daughter branches b_1 and b_2 which are generally asymmetrical with respect to branch dimension and volume of lung supplied by each daughter branch. Individual properties of branches are named analogical, e.g. A_1 and A_2 are the cross-sectional area of daughter branches. We considered 1453 branches, 727 of these are endpoints, below referred to as leaves of the tree. Every branch supports downstream a certain part of the total lung volume, its' so-called drain volume.

A key to the statistical description is the way in which the bronchial tree elements are numerically ordered. Traditional ordering assigns the trachea to the first order, the immediate daughter branches are second order and so on, a schema that is referred to as Weibel ordering. If asymmetric branching patterns prevail, branches having different diameter may have the same order, which produces inconsistencies in subsequent statistical evaluations. A different way is the Horsfield ordering [25], which starts at the most distal accessible branches and proceeds upwards. At merge points of branches having different orders the highest order of the daughter branch + 1 is assigned. The choice of the Horsfield order as appropriate grouping parameter is closely related to the observation that branching architecture and flow conditions are governed locally by the diameter of the bronchi [9,25–30]. Since we can assume that by the automated segmentation procedures all endpoints in the tree are about equally in size, these bronchi are reliable starting points to count upwards. The resulting Horsfield delta of a given branch, i.e. the difference in the orders assigned to its daughters, reflects an asymmetry in the geometry of the attached subtrees.

3. Statistical evaluation

In this section, we present a compact view on the statistical features of our lung model. A comprehensive discussion is given in Section 4.

3.1. Global structure

Fig. 3a shows the logarithm of the mean diameters and mean lengths of all bronchi of the reference model as a function of branching order. Definition of the order here and in all following figures follows the Horsfield ordering convention. Standard deviations are given from the first order on, with a mean length of 6.5 mm, and a mean diameter of 1.3 mm, up to the 15th order, for the two main stem bronchi (16th order) and the trachea (17th order) the standard deviation is not defined. Fig. 3b displays the relation of mean length against mean diameters. Fig. 3c plots the number of bronchi in relation to the branching

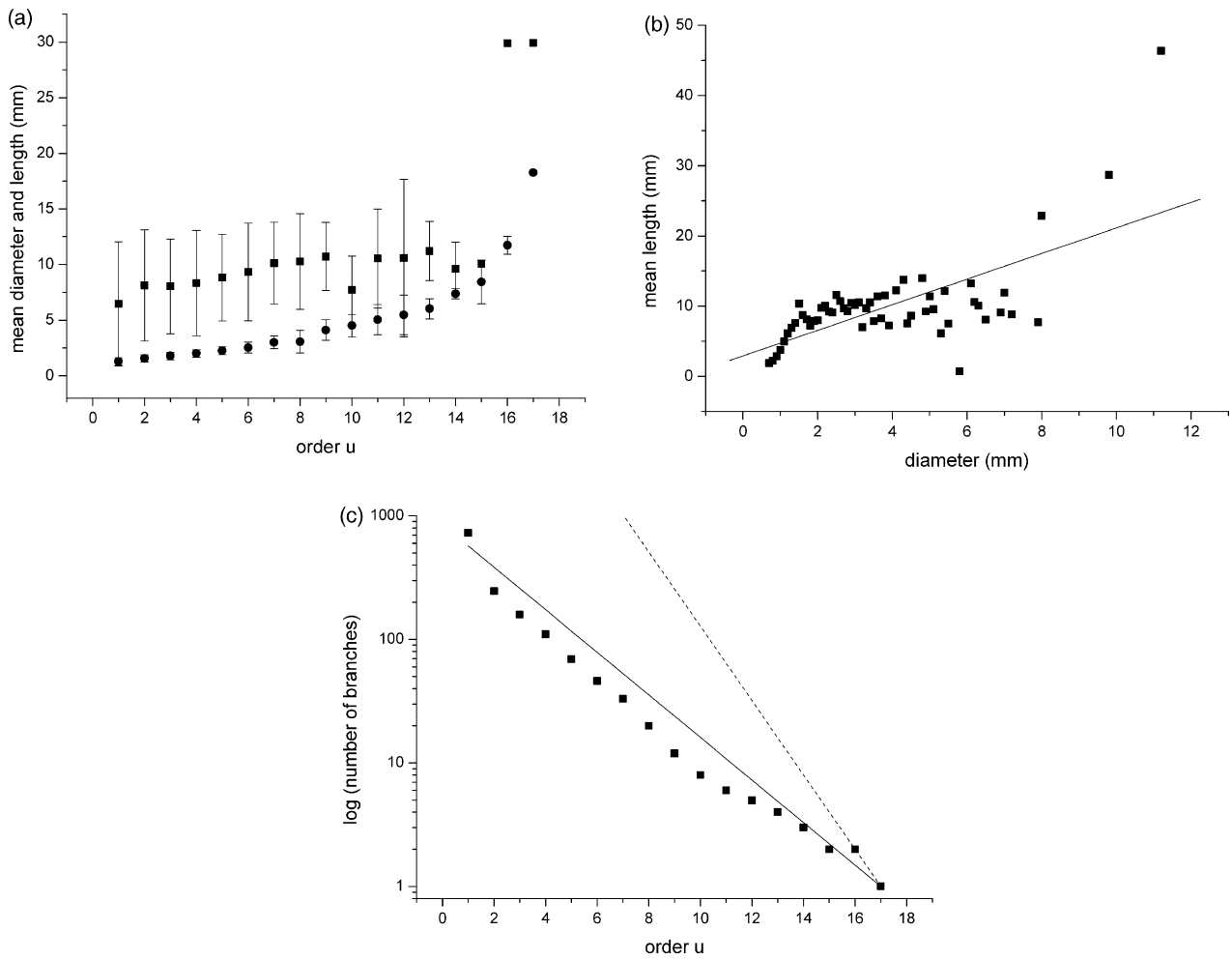

Fig. 3. (a) Mean diameters (round datapoints) and mean length (square datapoints) as function of Horsfield order. (b) Mean length (L) of branches of a given diameter (D). Diameters have been rounded to the the nearest 0.1 mm interval. The regression line fits the relation $L = 2.91 + 1.82D$. (c) Number of branches per Horsfield order on a logarithmic scale (square datapoints), which should be compared with that for a symmetrical system of 17 orders (dashed line). The regression line fits $n_{\text{branches}} = 1.48^{(17-u)}$, with an asymptotic standard deviation of 0.008.

order on a logarithmic scale. For reference the expected behaviour in case of symmetric branching is included.

3.2. Asymmetry

The results presented below demonstrate the asymmetry in the bronchial tree. Fig. 4a shows the frequency distribution of delta when Horsfield ordering is applied in each bifurcation. Bifurcations are grouped for the segments of the LU, left lower lobe (LL), right middle lobe (RM), right upper lobe (RU), and right lower lobe (RL). Fig. 4b is a display of the means of this differences delta per Horsfield order of the parent branch of the bifurcations. Fig. 4c shows the frequency distribution for the area asymmetry A_1/A_2 of daughter branches of area A_1 and A_2. Bifurcations are grouped according to the diameter of parent bronchi d_p. The set that fulfills the conditions 0.8 mm $< d_p <$ 2 mm and $d_p > 3.5$ is evaluated separate from the central part of the tree, which is 2 mm $< d_p <$ 3.5 *mm*. Fig. 4d demonstrates the relation between the area expansion A_1 plus A_2 against area of parent branch A_{parent}.

3.3. Scaling

We checked the bifurcation exponent x that determines the relation of parent and daughter branches $d_0^x = d_1^x + d_2^x$ (Fig. 5a). A total of 726 branches (1453 − 727 leaves) were analyzed. There were 18 branches with a bifurcation exponent greater than 15. Fitting a Gaussian distribution, the average was at 2.475 ± 0.046, $R^2 = 0.904$, and the arithmetic mean was 3.11 ± 5.12. One hundred and forty four of the branches did not satisfy the stringent bifurcation relationship.

To establish the existence of a multifractal scaling relationship we calculated a multifractal spectrum [31] given in Fig. 5b. The bronchi were grouped by Horsfield order u and for each bronchus a measure was established by $\mu_u(i) = \mathrm{d}_i / \sum_{i \in u} \mathrm{d}i$, where the sum runs over all bronchi of a given Horsfield order. The spectrum given in Fig. 5b reveals

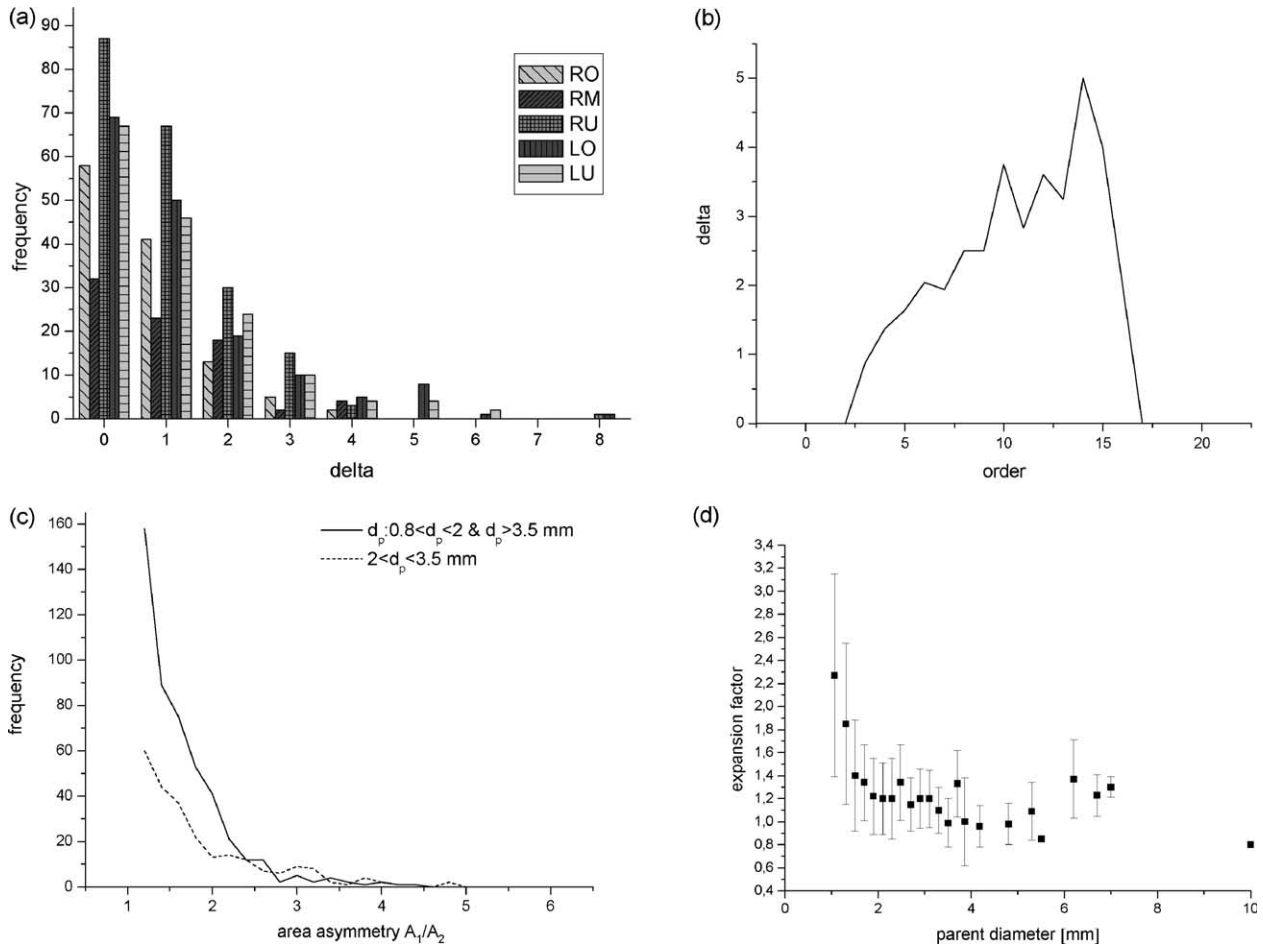

Fig. 4. (a) Frequencies for difference in the Horsfield ordering schema of daughter branches within different lung lobe segments. (b) Means for difference in order of daughter branches. (c) Frequency distribution for the area asymmetry A_1/A_2. The more asymmetric region of middle diameter range is evaluated separately. (d) Average expansion factor, i.e. ratio of combined daughter cross-sectional areas to parent cross-sectional area, as a function of parent diameter. The bars indicate one standard deviation above and below the mean.

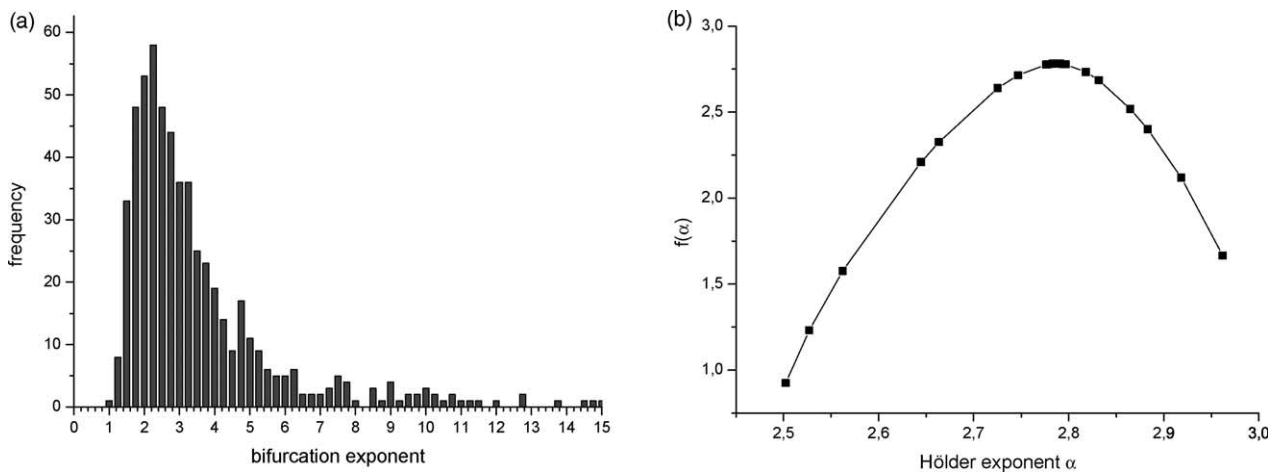

Fig. 5. (a) Distribution of the bifurcation exponent x that satisfies the relation $d_p^x = d_1^x + d_2^x$. (b) Multifractal spectrum of (coarse-grain) Hölder exponent α for a measure defined on the bronchi diameter. Bronchi are grouped according to the Horsfield order into groups of increasing scale.

this multifractal scaling property. The spectrum of the (coarse-grain) Hölder exponent α with respect to μ was calculated using an implicit method of moments as proposed in Ref. [32].

3.4. Volumetric implications

From the standpoint of function, the effect of asymmetry on gas distribution is of importance Therefore, we have analyzed the drain volume, which indicates the supplied total volume downstream. The drain volumes for each leaf were calculated according to Section 2.1. These volumes are propagated upwards to define the drain volume connected to each bronchus. The result we are providing here shows the drain volume related to the cross-sectional area (Fig. 6).

4. Discussion

The purpose of our investigation was to obtain more precise information of the bronchial tree by means of HRCT of in-vitro models and subsequent automated analysis. The airspaces of the lung are well suited for morphologic and morphometric analysis if they are accurately inflated and provide a contrast that is sufficiently enhanced for subsequent image analysis. Rubber cast models in conjunction with HRCT imagery are ideal for this purpose.

We compared the image volume resulting from the rubber cast with other in-vitro preparations, including lungs that were fixed using hot formalin vapor with a respirator modified for post-mortem formalin insufflation via the main bronchus. This technique, previously described as a volume-controlled fixation [33,34], was modified for pressure-controlled inflation using an 8-h ventilation cycle with inflation pressures up to a maximum of 40 cm H_2O. With the terminal airspaces fully inflated these specimen could be subsequently investigated by HRCT-scans (120 kV, 330 mA, 2 s, Somatom Plus, Siemens, Erlangen, Germany). With these preparations we could obtain a resolution of about 10 generations.

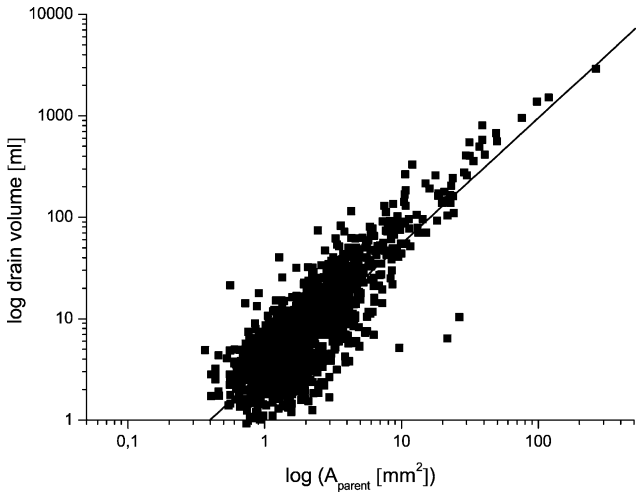

Fig. 6. Log of drain volume plotted against log of cross-section of parent branch. A linear fit on linearized scales, $(Y) = A + B(X)$, revealed $A = 0.497 \pm 0.014$, $B = 1.241 \pm 0.031$ regression coefficient $R = 0.723$, and a standard deviation of 0.398.

The software tools that were developed here are expected to improve clinical imaging, in particular for the automated analysis of the bronchial tree [35,36] considering the increased resolution provided by spiral and multislice CT. The methods are tuned towards a conservation of the topology of the original structure, the erosion is carried out symmetrically to provide a reliable and accurate central position of the skeleton and the boundary noise of the vessel surface does not lead to irrelevant skeleton lines that could be interpreted as side branches.

The reference model was established in different flavors. One form is that of a surface representation, suitable for computational fluid dynamics [37]. This data set contains subtle anatomical structures like regular imprints of the hyaline C-shaped cartilage rings around the trachea and the primary bronchi visible, these fine structures were not considered in previous CFD calculations. An abstracted form is that of a skeleton or graph that also includes information about the mean diameter of each branch. Such a graph contains sufficient geometrical information to run mass transport simulations [38,39]. Deviations from the anatomical exact shape exist in length, since the thinning algorithms reveal trajectories that follow the bounded shape of the bronchi, while the abstracted graph only contains start- and endpoint of each tube. This difference is diminishing downstream.

Global statistical evaluations confirmed previously published findings [18,25] such as the relation of the mean diameters as a function of branching order, as shown in Fig. 3a. The results presented here are good in line with the findings Horsfield and Cumming presented in Ref. [25]. For comparison the data have to be grouped by branching order, calculating regressing parameters a and b according to $\mathrm{d}(u) = ab^u$ for each group individual. We calculated for bronchi-branches with

order $u = 1–6$:

$a = 1.193 \pm 0.035$ and $b = 1.136 \pm 0.007$,

and for bronchus-branches

order $u = 7–16$:

$a = 0.965 \pm 0.175$ and $b = 1.162 \pm 0.015$.

For the branching order u is counting from below, to compare our findings with the results of Horsfield and Cumming the difference in branching order u had to be adjusted. Horsfield and Cumming described a tree with maximal order 25 while we present here results for a tree of maximal order 17, where the maximal order in both cases labels the trunk of the tree. Hence the groups given here correspond roughly with the two upper groups of Horsfield

and Cumming, for which they give values of $b = 1.062$ and $b = 1.161$, respectively.

As already mentioned in Section 2.1, the model presented here is reduced to a homogeneous hierarchical order for the whole lung. If we extend the hierarchical resolution for the right lung to an order in accordance with the data of Horsfield and Cumming, the regression analogue to Fig. 3b determines the relation of length to diameter only slightly different by $<2\%$ to previously published results from Horsfield and Cumming [25]. Since the increasing number of small-size bronchi dominates the results, the comparison of data with matched hierarchical depth is essential.

The number of bronchi in relation to the branching generations given in Fig. 3c reveals a regression of $1.48^{(\text{max. segmented order-}u)}$. Horsfield and Cumming [25] calculated the regression to be $1.38^{(\text{max. depth-}u)}$.

An important aspect of the overall design of the human bronchial tree is asymmetry. Looking at the area asymmetry in Fig. 4c, we see beside the center of the distribution at a value of 1.0 a clear asymmetric part. This asymmetry is most prominent for the bronchi with $2\text{ mm} < d_{\text{parent}} < 3.5$ mm. Hence, following the more or less symmetric first main bifurcations of the trachea a regime of enhanced asymmetric branches is noticeable. However, the outermost bifurcations reveal again a more symmetric behavior. So dichotomic and asymmetric bifurcations are mixed on all scales with a more asymmetric regime for $2\text{ mm} < d_{\text{parent}} < 3,5$ mm. This asymmetry of the individual bifurcations finds its counterpart in the structural asymmetry of the tree geometry revealed in Fig. 4a and b that represent the frequencies of differences in Horsfield order of the daughter branches of the bifurcations found in the tree. As the Horsfield order of a given bronchi characterises the depth of the adherent subtree, a difference in the Horsfield order of the daughter bronchi at a bifurcation reveals an asymmetry in the division of the parent tree into two subtrees at this bifurcation. Note that no major deviations in asymmetry were found when comparing the lung lobes. We cannot confirm the results of Phillips et al. [9], who reported that as the parent diameter decreases below 4 mm the expansion factor decreases, dropping to unity at a diameter of about 2.5 mm and remains around unity for parent diameters between 1.5 and 2.5 mm. As indicated in Fig. 4d, for parent diameters below about 2 mm the average expansion factor actually rises, reaching about 2.2 at 1 mm.

The bifurcation exponent x that determines the relation of parent and daughter branches $d_0^x = d_1^x + d_2^x$, is used to study self-organization in biological networks [38,39,40]. According to Mandelbrot [41] in case of a self similar tree this bifurcation exponent is to be closely related to the fractal dimension of the tree. In Fig. 5a the distribution shows a maximum at around a bifurcation exponent of 3, but has significant portions in the range between 2 and 4. The average, if fitted to a Gaussian distribution, gives $x = 2.475$. This is near to what other investigators have been determined, e.g. Bennet et al. [26] reported a bifurcation exponent of 2.36. We also determined the bifurcation exponent for each lung segment separately, but did not find any significant difference in the overall form of the distribution and location of the maximum. For dichotomic, symmetric and regular asymmetric models, the bifurcation exponent is a constant and closely related to the type of flow guided by the tree [26,30,35]. As a result, these designs predict homogenous flows and forces throughout the lung. This is in contrast to the spectrum in Fig. 5a, predicting a range of quite different flow conditions. For values <2 the cross-sectional area decreases and amplifies flow velocities, while $x = 4$ represents a constant fluid resistance with a preservation of pressure drop.

While the distribution given in Fig. 5a could be given for pure statistical reason, the existence of power-law like correlations showing up in the diameter scaling as shown above gives strong hints on the existence of a multifractal scaling relationship. To establish this, we analyze the scaling properties of the diameters with decreasing Horsfield order. Fig. 5b shows the resulting multifractal spectrum ensue from the analysis of Hölder exponents with Horsfield order u as scaling parameter. Hence the existence of multifractal scaling relationship tied to the spatial order induced by the branching of the tree is strongly suggested by our results, i.e. in case of the finite cluster given by the cast the multifractality is mainly induced to fat fractal of the branching system by the hierarchy of thicknesses [42]. As stated by Bennet et al. [26] the existence of such spectrum is evidence for self-affine multifractal properties of a branching network residing in a self-organized critical state. The asymmetric design has an impact on flow characteristics, but also on respiration if the drain volume is taken into account (Fig. 6). Drain volumes reveal deviations to larger or lower volumes in particular at mean orders, but converge towards higher orders.

5. Outlook

Any modeling and functional simulation of organs critically relies on the precision and representativeness of the structural models available. It was noted earlier that it is due to the lack of comprehensive morphological data of the human lung that the preferred model is the trumpet model [1,3]. With the availability of a realistic structural description and a more precise mapping of the lung architecture, simulations that concern the gas flow and particle deposition can now be performed with higher accuracy. The availability of a realistic computer representation of lung that can be scaled is an important step forward in lung research, toxicology and clinical applications including functional predictions. While scintigraphic predictions of ventilation are established in clinical routine, methods based on conventional CT-data are not since data only up to the seventh order is resolved. The goal of the presented

reference model is to fill in a larger portion of the bronchial tree that can be adapted accordingly to carry out such individual predictions based on CT-data. Work is in progress to add patient architectural information of downstream bronchioli and respiratory units that can complement this representation.

6. Additional data file

An abstracted graph describing the bronchial tree topology as presented in this paper is available from the authors upon request.

7. Summary

We describe the development of a digital reference model of the bronchial tree of the human lung based on an in-vitro preparation. A rubber cast model based on a fully inflated normal human lung was imaged using HRCT. The resolution obtained with this specimen was superior to other in-vitro preparations and data sets obtained by clinical imaging, due to the absence of bones and tissue that limit contrast, absence of motion artifacts, and the high degree of the radiation dose applicable. A new set of image processing tools was developed and applied to derive various abstracted representations suitable for statistical investigation and simulation. An abstracted topological graph contained 1453 bronchi up to the 17th generation. A post-processing step resolved ambiguities in the branching pattern of the graph. The model revealed geometric–statistical and fractal properties and were compared with current models. Results support a model that exhibits strong asymmetry and multifractal properties.

Acknowledgements

We like to thank P. Gehr from the Institute of Anatomy at the University of Bern, Switzerland, and H. Schulz from the GSF-National Research Center for Environment and Health, Neuherberg, Germany, for the provision of the rubber cast of the lung and the tomographic data, respectively. We are indebted to our colleague Florian Link for his excellent work on the ILAB4 Framework. This work was supported by DFG, project # KR 1921/2-1 and HOP 1921/2-2.

References

[1] Lazaridis M, Broday DM, Hov O, Georgopoulos P. Integrated exposure and dose modeling and analysis. 3. Deposition of inhaled particles in the human respiratory tract. Environ Sci Technol 2001;35:3727–34.
[2] Fleming JS, Nassim M, Hashish AH, Bailey AG, Conway J, Holgate S, Halson P, Moore E, Martonen TB. Description of pulmonary deposition of radiolabeled aerosol by airway generation using a conceptual three dimensional model of lung morphology. J Aerosol Med 1995;8(4):317–27.
[3] Schroeter JD, Fleming JS, Hwang D, Martonen TB. A computer model of lung morphology to analyze SPECT images. Comp Med Imaging Graphics 2002;26:237–46.
[4] Kitaoka H, Takaki J, Suki B. A three-dimensional model of the human airway tree. J Appl Physiol 1999;87(6):2207–17.
[5] Weibel ER. Morphometry of the human lung. Berlin: Springer; 1963.
[6] Yeh HC, Schum GM. Models of human lung airways and their application to inhaled particle deposition. Bull Math Biol 1980;42:461–80.
[7] Schlesinger RB, McFadden L. Comparative morphometry of the upper bronchial tree in six mammalian species. Anat Rec 1981;199:99–108.
[8] Patra AL. Comparative anatomy of mammalian respiratory tract: the nasopharyngeal region and the tracheobronchial tree. J Toxicol Environ Health 1986;17:163–74.
[9] Phillips CG, Kaye SR. On the asymmetry of bifurcation in the bronchial tree. Respir Physiol 1997;107:85–98. Phillips CG, Kaye SR, Schroter RC. A diameter-based reconstruction of the branching pattern of the human bronchial tree. Part I. Description and application. Respir Physiol 1994;98:193–217.
[10] Balashazy I, Hofmann W, Heistracher T. Computation of local enhancement factors for the quantification of particle deposition patterns in airway bifurcations. J Aerosol Sci 1999;30:185–203.
[11] Martonen TB, editor. Medical applications of computer modelling—the respiratory system. Advances in computational bioengineering, vol. 4. WIT Press; 2001.
[12] Darquenne C. A realistic two-dimensional model of aerosol transport and deposition in the alveolar zone of the human lung. J Aerosol Sci 2001;32(10):1161–74.
[13] Martonen TB, Musante CJ, Segal RA, Schroeter JD, Hwang D, Dolovich MA, Burton R, Spencer RM, Fleming JS. Lung models: strengths and limitations. Respir Care 2000;45(6):712–36.
[14] Koblinger L, Hofmann W. Monte Carlo Modelling of aerosol deposition in human lungs. Part I: Simulation of particle transport in a stochastic lung structure. J Aerosol Sci 1990;21:661–74.
[15] Howatson-Tawhai M, Hunter PJ. Simulating gas transport in an anatomically-based mathematical model of the human lungs In: BED, vol. 50, 2001 Bioengineering Conference, ASME; 2001. p. 89–90.
[16] Lazaridis M, Broday DM, Hov O, Geogropoulos PG. Integrated exposure and dose modeling and analysis system. 3. Deposition of inhaled particles in the human respiratory tract. Environ Sci Technol 2001;35(18):3727–34.
[17] Weibel ER. Personal communications, 2003.
[18] Lorensen WE, Cline HE. Marching Cubes: a high resolution 3D surface reconstruction algorithm. Comp Graphics 1987;21(4):163–9.
[19] Selle D, Spindler W, Preim B, Peitgen H-O. Mathematical methods in medical imaging: analysis of vascular structures for liver surgery planning. In: Engquist B, Schmid W, editors. Mathematics unlimited—2001 and beyond. Berlin: Springer; 2000. p. 1039–59.
[20] Krass S, Selle D, Boehm D, Jend H-H, Kriete A, Rau W, Peitgen H-O. A method for the determination of bronchopulmonary segments based on HRCT data. Computer assisted radiology and surgery (CARS 2000), San Francisco. Amsterdam: Elsevier Science; 2000. p. 584–9.
[21] Hahn HK, Preim B, Selle D, Peitgen H-O. Visualization and interaction techniques for the exploration of vascular structures. Proceedings of IEEE visualization. 2001. p. 395–402.
[22] Selle D, Peitgen H-O. Analysis of the morphology and structure of vessel systems using skeletonization. In: Chen C-T, Clough AV, editors. SPIE medical imaging 2001. Proceedings of SPIE, San Diego, vol. 4321; 1968. p. 271–81.

[23] Kuhnigk J-M, Hahn HK, Hindennach M, Dicken V, Krass S, Peitgen H-O. Lung lobe segmentation by anatomy-guided 3D watershed transform. In: Sonka M, Fitzpatrick JM, editors. Medical imaging 2003: image processing. Proceedings of SPIE 2003, vol. 5032.; 2003. p. 1482–90.
[24] Schröcker F, Berghorn W, Bettag H, Bohne A, Breitenborn J, Hahn H, Preim B, Rascher-Friesenhausen R, Schenk A, Selle D, Spindler W, Jürgens H, Lang M, Peitgen H-O. Highly integrated user-friendly research and development platform for medical image processing and visualization. Radiol Suppl 2001;217:699.
[25] Horsfield K, Cumming C. Morphology of the bronchial tree in man. J Appl Physiol 1968;24:373–83.
[26] Bennet SH, Eldridge MW, Puente CE, Riedi RH, Melson TR, Goetzman BW, Milstein JM, Singhal SS, Horsfield K, Woldenberg MJ. Origin of fractal branching complexity in the lung, Whitepaper of the University of California, 2001.
[27] Uylings HBM. Optimization of diameters and bifurcation angles in lung and vascular tree structures. Bull Math Biol 1977;39:509–20.
[28] Weibel ER. The pathway of oxygen. Cambridge: Harvard University Press; 1984.
[29] Kitaoka H, Takahashi T. Relationship between the branching pattern of airways and the spatial arrangement of pulmonary acini – a re-examination from a fractal point of view. In: Nonnenmacher TF, Losa GA, Weibel ER, editors. Fractals in biology and medicine. Birkhaeuser, Basel; 1994. p. 116–31.
[30] Horsfield K, Thurlbeck A. Relation between diameter and flow in branches of the bronchial tree. Bull Math Biol 1981;43(6):681–91.
[31] Evertsz CJG, Mandelbrot BB. Multifractal measures. In: Peitgen H-O, Jürgens H, Saupe D, editors. Chaos and fractals. New York: Springer-Verlag; 1992. p. 921–53. Appendix B.
[32] Chhabra A, Jensen RV. Direct determination of the f(a) singular spectrum. Phys Rev Lett 1989;62(12):1327–30.
[33] Mittermayer C, Wybitul K, Rau WS, Ostendorf P, Riede UN. Standardized fixation of human lung for radiology and morphometry; Description of a 'two chamber'-system with formaldehyde vapor inflation. Pathol Res Pract 1978;162(1):115–30.
[34] Rau WS, Mittermayer C. Volume controlled fixation of the lung by formalin vapor. ROFO Fortschr Geb Rontgenstr Nuklearmed 1980; 133(3):233–9.
[35] Schlathölter T, Lorenz C, Carlsen IC, Renisch S, Deschamps T. Simultaneous segmentation and tree reconstruction of the airways for virtual bronchoscopy. In: Sonka M, Fitzpatrick JM, editors. Medical imaging 2002: image processing. Proceedings of SPIE 2002, vol. 4684.; 2002. p. 103–13.
[36] Ley S, Mayer D, Brook B, van Beek EJR, Heusell CP, Hose DR, Rinck D, Kauczor HU. Radiological imaging as the basis for a simulation software to advance individualised inhalation therapies. Eur Radiol 2001;11(Suppl):216–7.
[37] Kunz RF, Haworth DC, Leemhuis LS, Davison AC, Zidowitz S, Kriete A. Eulerian multiphase CFD analysis of particle transport and deposition in the human lung. Proc Biomed 2003.
[38] Kriete A. Form and function of lung: analysis by scientific image computing. Monography, Springer series in anatomy, embryology and cell biology, vol. 145. Berlin: Springer; 1998.
[39] Mercer RR, Anjilvel S, Miller FJ, Crapo D. Inhomogeneity of ventilatory unit volume and its effects on reactive gas uptake. J Appl Physiol 1991;70(5):2193–205.
[40] Uylings HBM. Optimization of diameters and bifurcation angles in lung and vascular tree structures. Bull Math Biol 1977;39:509–20.
[41] Mandelbrot BB. The fractal geometry of nature. New York: W.H. Freeman and Company; 1983.
[42] Jestczemski F, Sernetz M. Multifractal approach to inhomogeneous fractals. Physica A 1996;233(3–4):275–82.

Andreas Schmidt holds a master (Diploma) in Physics and is a research associate at the Department of Anatomy and Cell Biology, University of Giessen. He leads the group in aspects of computer modeling and simulation of the human lung at the department and is currently involved in applying methods to calculate mass transport and flow including Navier–Stokes equations.

Thorsten Denhard is a graduate in computer science at the UAS in Giessen. He is a professional practical at the Department of Anatomie and Cell Biology, University of Giessen, and developed a set of software-tools for the statistical analysis and numerical simulation in course of the lung project.

Andres Kriete has a PhD in physics (1986) and is Associate Professor for Bioinformation Engineering at the School for Biomedical Engineering, Science and Health Systems at Drexel University in Philadelphia. He was Director of Imaging Sciences and Bioinformatics at TissueInformatics. Inc., Pittsburgh, and visiting professor at the Bioengineering Department at the University of Pittsburgh from 2001–2003 and Head of the Image Processing Laboratory at the University Clinic in Giessen from 1987 to 2000. He is involved in R & D projects that include automated multidimensional imaging, image analysis, biocomputing and bioinformatics.

Stephan Zidowitz earned his PhD in Physics from the Technical University Carolo-Wilhelmina at Braunschweig, Germany, in 1997. He is staff member of the Center for Medical Diagnostic Systems and Visualisation, Bremen, working on medical image processing and analysis. Currently he is working on the development of software assistants for the analysis of thoracic CT-data for clinical use.

Stefan Krass obtained his MS in physics (1992) and his PhD in physiology (1997) from the Johannes Gutenberg University Mainz, Germany. Currently he is research associate of the Center for Medical Diagnostic Systems and Visualization, Bremen, working primarily in the area of computer assistance for thoracic radiology.

Heinz-Otto Peitgen holds a Chair in mathematics at the University of Bremen, Bremen, Germany, where he is Director of the Center for Complex Systems an Visualization. He is also Professor of Mathematics and Biomedical Science at the Florida Atlantic University, Boca Raton. In 1995, he founded the Center for Medical Diagnostic Systems and Visualisation, Bremen, which he chairs as CEO. His scientific expertise is in dynamical systems, numerical analysis, computer graphics, scientific visualization, image and data analysis and processing, and computer-aided radiology.